

Incomplete fusion calculations in the $^{27}\text{Al}(^{16}\text{O},xy)$ reaction at 65, 77, and 87.4 MeV bombarding energies

S. J. Padalino and L. C. Dennis

Department of Physics, Florida State University, Tallahassee, Florida 32306

(Received 26 December 1984)

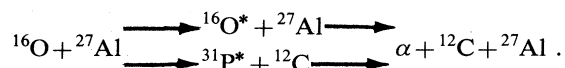
Angular correlations have been investigated in the $^{27}\text{Al}(^{16}\text{O},xy)$ reaction at 77 MeV. Using a ^{31}P intermediate mechanism to model the interaction, attempts have been made to predict the $\alpha + ^{12}\text{C}$ angular correlations at 65, 77, and 87.4 MeV. The calculations reproduce the shape of the correlations fairly well. However, the predicted angular correlation peaks too far out in angle to reproduce the experimental data. Several possible explanations for the shifting of the peaks are discussed.

I. INTRODUCTION

Projectile breakup occurs in many heavy ion collisions.¹⁻¹⁰ The signature of this process can be seen in the velocity spectra of projectilelike fragments which are dominated by broad peaks centered about the beam's velocity.^{1,2} Projectile fragments can be discerned from fusion residues of the same mass by their velocities.¹¹ Thus, for two-body final states, the fragmentation process is indicative of particle transfer. However, it has been shown that at energies as low as 5 MeV/nucleon projectile breakup can occur, whereby neither projectile fragment is captured by the target.³

In order to gain a better understanding of the projectile breakup process in the $^{27}\text{Al}(^{16}\text{O},xy)$ reaction, it was necessary to perform coincident measurements. The ^{16}O projectilelike fragments N and C were detected inclusively and in coincidence with protons and alpha particles. Fragment pairs p-N and α -C were analyzed since they could reconstruct the mass of the beams.

Two possible mechanisms which produce α -C coincidence are shown in the following:



The first of these mechanisms can be described as inelastic breakup (IB), where the projectile is inelastically excited above the α - ^{12}C threshold, allowing the $^{16}\text{O}^*$ to break up. In this case the target plays a spectator role. The second mechanism is characterized as a two-step transfer-evaporation process (incomplete fusion, IF), whereby an alpha particle is transferred to the ^{27}Al forming $^{31}\text{P}^*$, which then alpha decays from an equilibrated compound nucleus. The IB and IF mechanisms can both contribute to the ^{12}C inclusive cross section.

Coincidence measurements in the $^{27}\text{Al}(^{16}\text{O},\alpha^{12}\text{C})$ reaction have been investigated by other groups.³⁻⁶ Their work suggests that, the bombarding energy and possibly the carbon detection angle, strongly enhance the ability to observe inelastic breakup. The coincidence measurements of these other studies have all been made with the ^{12}C detector set well behind the grazing angle. Table I con-

tains a list of grazing angles and detection angles of past studies.

Although our work at 77 MeV is at a different energy than earlier studies,³⁻⁵ the significant difference between this work and other investigations is in the placement of the heavy ion detector which is well within the grazing angle. It has been seen by Sasagase *et al.*³ that α - ^{12}C correlations produced via inelastic breakup were made by detecting alpha particles over a forward angular range of -15° to 10° . It was hoped that if inelastic breakup occurred at 77 MeV it might be more easily seen over an angular range of $+20$ to $+40$ deg if the ^{12}C detector was placed inside of the grazing angle.

Data acquisition and collection are discussed in Sec. II and the motivation and results for the incomplete fusion calculations are given in Secs. III and IV. A comparison between the experimental and predicted results is addressed in Sec. V, and a general overview of the projectile fragmentation process in the 65 to 87.4 MeV bombarding energy range is given in Sec. VI.

II. EXPERIMENTAL PROCEDURE

The experiment was performed using the Florida State University Super FN Tandem Accelerator, which produced a beam of 77 MeV ^{16}O 8^+ ions. The beam was

TABLE I. The carbon detector angles of several studies are displayed along with the grazing angles for each energy.

Energy (MeV)	^{12}C θ	θ_{gr}
65 ^a	30°	24°
65 ^b	30°	24°
77 ^c	15°, 30°	20°
87.4 ^d	20°, 30°	17°
100 ^e	30°	13°
144 ^f	8.75°, 13°	

^aReference 4.

^bReference 5.

^cThis work.

^dReference 3.

^eReference 16.

^fReference 6, ^{28}Si target.

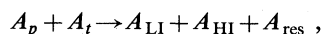
40–130 nA on target. The relatively large beam intensity is attributed to the second beam stripper positioned midway between the terminal and the end of the high energy column. Self-supporting ^{27}Al foils, 1.2 mg/cm^2 in thickness, were used as targets.

Six conventional ΔE - E telescopes were used to detect heavy ions and light ions in both coincidence and singles modes. Four telescopes were dedicated to detect light ions (LI) $1 \leq Z \leq 2$. They were mounted in 9 deg intervals on a movable wedge. Each telescope in the wedge consisted of a $40 \mu\text{m}$ ΔE Si surface barrier detector and a $2000 \mu\text{m}$ SiLi detector. The two heavy ion detectors were mounted at fixed positions of 15 and 30 deg in the laboratory. These telescopes detected particles with $3 \leq Z \leq 8$. Both telescopes were composed of a $15 \mu\text{m}$ ΔE and a $100 \mu\text{m}$ E Si surface barrier detector. Aluminum foil was placed over the light ion telescopes to absorb the elastically scattered ^{16}O . Solid angles ranged from 0.4 to 6 msr during the course of the experiment.

Angular correlations measurements were made by allowing either of the two fixed heavy ion (HI) telescopes, at 15° and 30° , to be in coincidence with any one of the four LI telescopes which were placed at 9° intervals over an angular range of 50 to -63 deg. Event timing was done externally to the acquisition computer. Timing circuits produced time-to-amplitude converter (TAC) spectra which allowed a means of monitoring the real to random ratio which ranged between 50 to 100. This same circuit generated logic gate pulses which fired the analog-to-digital converter (ADC) processing. Event data were then collected and stored on magnetic tapes and reduced off line at a later time.

III. KINEMATICS

Two convenient variables which are often used to describe three-body kinematics are the three-body Q value, Q_3 , and the relative kinetic energy E_{rel} . These variables are chosen to simplify the representation of the three-body kinematics and to give better insight into the three-body problem. Consider the reaction where a projectile (p) collides with a target (t) producing a three-body final state consisting of a light ion (LI), a heavy ion (HI), and a residual (res):



if, the energies and the angles of the heavy ion and light ion are known, then by using conservation of energy and momentum the Q_3 value can be determined.

$$\mathbf{P}_{\text{beam}} = \mathbf{P}_{\text{res}} + \mathbf{P}_{\text{HI}} + \mathbf{P}_{\text{LI}}, \quad (1)$$

$$E_{K,\text{beam}} = E_{K,\text{res}} + E_{K,\text{HI}} + E_{K,\text{LI}} - Q_3. \quad (2)$$

Using Eqs. (1) and (2), the energy and angle of the residual and the Q_3 value can be calculated. A Q_3 spectrum (Fig. 1) can be produced by calculating Q_3 values for different events which were measured at the same HI and LI angles. Three subscripted indices (Q_{kij}) identify the excited states in each of the exciting nuclei. For example, in the reaction $^{27}\text{Al}(^{16}\text{O}, \alpha)^{12}\text{C}^{27}\text{Al}$, $Q_3 = Q_{ggg}$ would indicate that the ^{12}C and ^{27}Al nuclei were in their ground states.

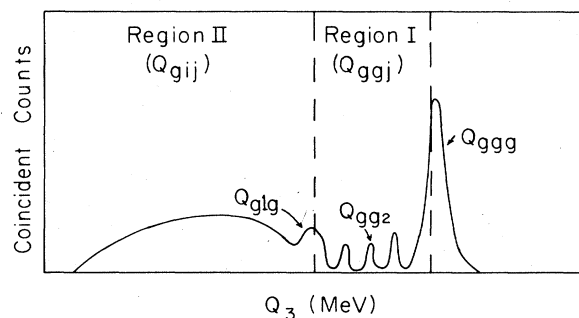


FIG. 1. A schematic Q_3 spectrum containing three-body final states which were produced exclusively by excitations in the residual are displayed in region I. Region II contains Q_3 peaks produced from both heavy ion and residual excitations.

A schematic of the Q_3 spectrum is shown in Fig. 1. Region I is designated by Q_{ggj} which represent Q_3 peaks which are only produced from excited states in ^{27}Al . Region II begins where the first excited state in ^{12}C produces a Q_3 peak (Q_{glg}). Q_3 values more negative than Q_{glg} represent excitations in both the ^{12}C and ^{27}Al . However, when two or more three-body final states have the same Q_3 value the labeling of the Q_3 peaks becomes ambiguous.

The relative kinetic energy between $\alpha + ^{12}\text{C}$, $^{12}\text{C} + ^{27}\text{Al}$, and $\alpha + ^{27}\text{Al}$ pairs can be determined experimentally for a known three-body final state. The excitation energies of the ^{12}C and ^{27}Al are fixed by choosing events which only occur in a specific Q_3 peak. The relative kinetic energy for each of the three pairs can be plotted as a function of alpha detection angle.

From the relative kinetic energy plot inferences can be made as to which intermediate nucleus produced the pair. If a particular pair of exiting nuclei exhibit a constant relative kinetic energy over an angular range then it is possible that the pair was produced from an intermediate nucleus which was originally composed of the masses of the pairs. However, in the case of the $\alpha + ^{27}\text{Al}$ pair it is a necessary condition for the relative kinetic energy to be constant over the entire angular range in order for the pair to have been formed by the ^{31}P intermediate state. This result occurs because the ^{12}C detector is fixed and has a finite solid angle. The fixed solid angle inhibits the detection of the full angular range of the $\alpha + ^{12}\text{C}$ and $^{12}\text{C} + ^{27}\text{Al}$ pairs but not the $\alpha + ^{27}\text{Al}$ pair.

If the $\alpha + ^{27}\text{Al}$ pair does maintain a constant value over the entire angular range it can be inferred that the ^{31}P intermediate state produced the pair. For $Q_3 = Q_{ggg}$ events the excitation energy of the ^{31}P state is related to the relative kinetic energy by

$$E_x = E_{\text{rel}} + E_{\text{threshold}},$$

where $E_{\text{threshold}}$ is the separation energy required for the breakup of the ^{31}P nucleus into an $\alpha + ^{27}\text{Al}$. Thus, the relative kinetic energy between the $\alpha + ^{27}\text{Al}$ can be used to determine the excitation energy of the ^{31}P prior to breakup.

Some earlier experimental evidence⁴ suggests that at

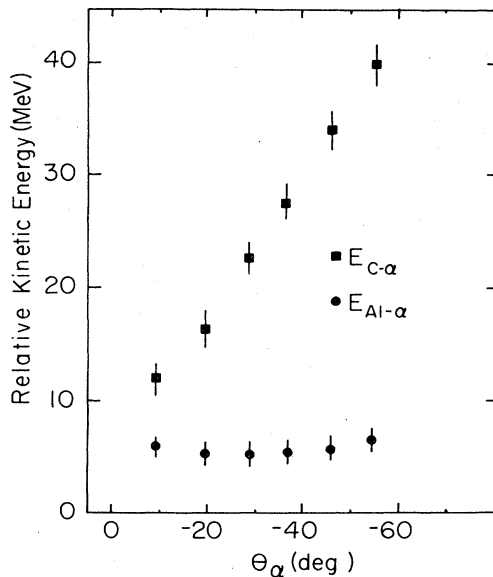


FIG. 2. The measured relative kinetic energy between $\alpha + {}^{12}\text{C}$ and $\alpha + {}^{27}\text{Al}$ pairs.

bombarding energies of less than 80 MeV the α - ${}^{12}\text{C}$ pair production is formed through the ${}^{31}\text{P}$ intermediate state. The relative kinetic energy of the most likely state in this energy range has been found to be $E_x = 14.5$ MeV.^{4,5} The measured relative kinetic energy between the $\alpha + {}^{27}\text{Al}$ pair, at 77 MeV bombarding energy, is constant within experimental error over the angular range shown in Fig. 2. However, the α - ${}^{12}\text{C}$ relative kinetic energy changes dramatically over this range (Fig. 2). This indicates that the alpha particles could have been formed from the ${}^{31}\text{P}$ reference frame at an excitation energy of $E_x = 15$ MeV.

IV. CALCULATIONS OF ANGULAR CORRELATIONS

The measurements reported here and those of other investigators³⁻⁵ have motivated us to model the reaction process as an incomplete fusion process. In order to produce $\alpha + {}^{12}\text{C}$ coincidences in an incomplete fusion reaction it is necessary to treat the reaction as a three-step process, wherein the projectile breaks up in the vicinity of the target, one of the two projectile fragments fuses with the target forming a compound nucleus which decays via statistical emission of light particles. To compare this model with experimental distributions requires a knowledge of the breakup process, the fusion process, and the subsequent evaporation cascade from an excited compound nucleus. The requirements of the evaporation cascade dictate that at least part of the calculation be Monte Carlo in nature. The starting point of the evaporation cascade for this reaction is ${}^{31}\text{P}$. Its subsequent decay was determined by statistical model calculations which depend upon the velocity, excitation energy, and total angular momentum of the ${}^{31}\text{P}$. In the approach described below we used the ${}^{12}\text{C}$ inclusive spectrum and conservation of momentum and energy to determine the number of ${}^{31}\text{P}$ nuclei with a

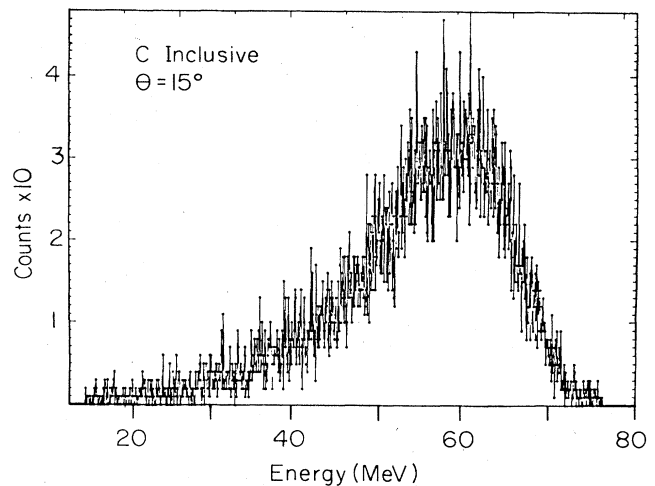


FIG. 3. The C inclusive spectrum measured at 15° (bombarding energy of 77 MeV).

particular velocity, excitation energy, and total angular momentum. These starting conditions for the ${}^{31}\text{P}$ nuclei were used as input to a Monte Carlo Hauser-Feshbach calculation (MCHF). The MCHF decay sequences were kinematically traced into the laboratory frame on an event-by-event basis. This event-by-event information was stored on a disk and then sorted into angular correlations as needed.

The ${}^{12}\text{C}$ inclusive spectrum shown in Fig. 3 was used to determine the direction of the recoiling ${}^{31}\text{P}$ and its excitation energy (Fig. 4). The relative population of states in ${}^{31}\text{P}$ is determined by the corresponding intensity in the ${}^{12}\text{C}$ inclusive spectrum (Fig. 3). This correspondence between the ${}^{31}\text{P}$ directions and excitation energies and the energy of the C ions was calculated by two-body kinematics assuming that all of the observed ions are ${}^{12}\text{C}$ nuclei which were produced in their ground state. The assump-

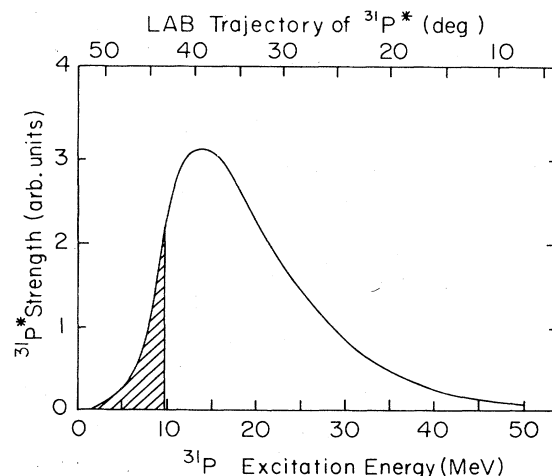


FIG. 4. ${}^{31}\text{P}^*$ states which are generated from the ${}^{12}\text{C}$ inclusive spectrum (Fig. 3). The upper scale indicates the laboratory direction of the ${}^{31}\text{P}^*$ prior to breakup.

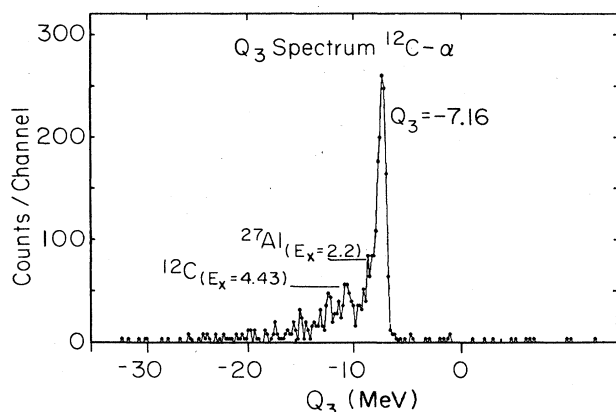


FIG. 5. The Q_3 spectrum determined from the $\alpha + {}^{12}\text{C}$ coincidences. The $Q_3 = -7.16$ peak indicates a three-body final state $\alpha + {}^{12}\text{C}_{\text{g.s.}} + {}^{27}\text{Al}_{\text{g.s.}}$. The -11.59 and -9.36 peaks represent the three-body final states $\alpha + {}^{12}\text{C}_{(e_x=4.43)}^* + {}^{27}\text{Al}_{\text{g.s.}}$ and $\alpha + {}^{12}\text{C}_{\text{g.s.}} + {}^{27}\text{Al}_{(e_x=2.2)}^*$, respectively.

tion that all of the nuclei are produced in their ground state is not too unreasonable if one considers the strength of the -7.16 MeV band in the Q_3 spectrum, shown in Fig. 5. The effect of adding excited states of ${}^{12}\text{C}$ or adding other C isotopes into the calculation will be discussed below.

Determination of the initial angular momentum distribution of the states in ${}^{31}\text{P}$ was based on the sharp cutoff model¹² for the fusion of an alpha particle moving at the beam velocity with ${}^{27}\text{Al}$. Thus, only the states with a total angular momentum J , such that $J \leq l_{\text{max}} + s_{\text{Al}}$ (s_{Al} is the ground state spin of ${}^{27}\text{Al}$), were included in ${}^{31}\text{P}$. The relative strengths of the allowed angular momentum values were determined as follows:

$$P(J) = \frac{\sum_{l=|J-s|}^{l_{\text{max}}} (2l+1)}{\sum_J \sum_l (2l+1)}, \quad (3)$$

where $P(J)$ is the probability for a state with total angular momentum J to be populated in ${}^{31}\text{P}$. The sum on l extends over all l values which are allowed by angular momentum coupling and are less than l_{max} .

The second step of the calculation is performed using the ${}^{31}\text{P}$ excitation energy and angular momentum distributions as input. Once the excitation energy and angular momentum of the ${}^{31}\text{P}$ is known it is possible to follow the particle decay sequence of this excited nucleus until insufficient energy remains for further decay. The formalism for such a Monte Carlo calculation is given by Gomez del Campo *et al.*¹¹ The limitation of allowable decay products to neutrons, protons, and alphas, and the parametrization of level densities and transmission coefficients used in this work are taken from LILITA.¹¹ The computer algorithm used here for the evaporation sequence differs from that of Ref. 11. In an attempt to reduce the required calculation time, the code used here saves partial decay sequences while LILITA does not. This technique will save

time only if a large number of events are required. The decay sequences, including the angular momenta involved, are saved on an event-by-event basis. This allows for separate calculations of the evaporation cascade and the kinematics. The decoupling of kinematics and statistical decay allows for a more complete sampling of the angular distribution.

The final step of the calculation determines the laboratory energy and angular distribution of the evaporation products from the event-by-event data. This is done by randomly selecting the direction of emission of the decay particle and then determining the direction of the recoil by momentum conservation. This process is repeated until the end of the evaporation sequence is reached. The event-by-event formalism is also given by Gomez del Campo *et al.*¹¹

There are many factors which could affect the validity of this type of calculation, even if one does not consider possible inadequacies of the model on which the calculation is based. For this reason several variations of the parametrizations and required initial distributions were tried. In particular, the sensitivity of the predicted angular correlations to the residual nuclei's level density parameters, the protons, neutrons, and alpha transmission coefficients, the ${}^{31}\text{P}$ initial angular momentum distribution, the initial ${}^{31}\text{P}$ excitation energy distribution, and the angular distribution of the light decay products was tested. As with other evaporation calculations, the predicted number of protons, neutrons, and alphas depends strongly upon all of these factors. However, the angular correlation depends primarily upon the initial excitation energy (and therefore the initial angular distribution) of the ${}^{31}\text{P}$. The ${}^{31}\text{P}$ angular distribution is determined by the measured ${}^{12}\text{C}$ energy distribution and two-body kinematics. The reason for the insensitivity of the location of the angular correlation peak to other parameters is due to the symmetric decay of the light particles about the primary ${}^{31}\text{P}$ direction. Most of the parameters in the calculation will affect the angular distribution of alpha particles about the ${}^{31}\text{P}$ direction, but the ${}^{31}\text{P}$ angular distribution fixes the location of the peak in the correlation spectrum.

The shaded area in the ${}^{31}\text{P}$ spectrum (Fig. 4) represents a range of excitation energies which were produced exclusively through alpha transfer. This range corresponds to ${}^{12}\text{C}$ nuclei with energies greater than 66 MeV; this corresponds to excited states in ${}^{16}\text{O}$ which are below the α - ${}^{12}\text{C}$ threshold. Thus, IB is forbidden by energy conservation in this energy range.

The shape of the angular correlations is strongly influenced by the choice of ${}^{31}\text{P}$ excitation energy distributions and by the angular distribution of the outgoing neutron, protons, and alpha particles in the ${}^{31}\text{P}$ reference frame. A mixture of isoplanar and planar¹³ distributions was used in the predictions. The actual distribution falls somewhere between the two, but it is not a linear combination of the two. Figures 6(a) and (b) demonstrate the effect on the angular correlation when pure planar or pure isoplanar was used in the ${}^{31}\text{P}$ frame. As a first estimate of the actual distribution, different admixtures of both planar and isoplanar distributions were tried. It was found that a 10% isoplanar and 90% planar distribution best predicted

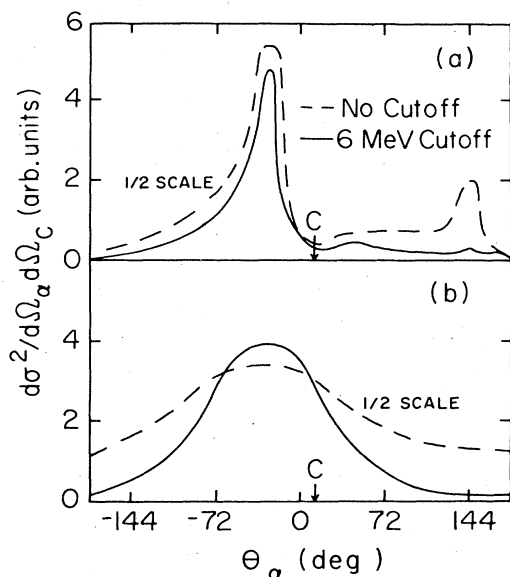


FIG. 6. The dotted curves are the predicted angular correlation which results from a pure planar (a) and pure isoplanar (b) α evaporation distribution in the ^{31}P reference frame. The solid curve is the same calculation with a 6 MeV cutoff. The dashed curves have been multiplied by $\frac{1}{2}$ so their shapes can be easily compared to the solid curves.

the shape of the angular correlation. Experimentally, the low energy cutoff of the detector telescopes affect the shape of the angular correlation. This effect can be accounted for in the calculation by excluding those coincidences with alpha energies less than 6 MeV [Figs. 6(a) and (b)]. The low energy cutoff affects the angular correlation by reducing the width of the forward peak. At lower bombarding energies the cutoff can eliminate the backward peaks in the planar distributions [Fig. 6(a)]. A further consideration of the low energy cutoff can be seen in the dramatic drop in the magnitude of the angular correlation cross section. A 6 MeV cutoff halves the height of the forward peak; a 12 MeV cutoff was found to half it again. The experimental cutoff is approximately 7 MeV.

V. DISCUSSION AND RESULTS

Angular correlation measurements of the $\alpha + ^{12}\text{C}$ pair, which were made by Harris *et al.*,⁴ Tsang *et al.*,⁵ Sasagase *et al.*³ and this work, are shown in Fig. 7. All four correlations were made in the scattering plane defined by the beam and the outgoing ^{12}C . The ^{12}C detection angle for each correlation is designated by an arrow in Fig. 7. The correlations, in Figs. 7(c) and (d) contain $\alpha + ^{12}\text{C}$ pairs produced by the entire Q_3 spectrum. Figures 7(a) and (b) contain $\alpha + ^{12}\text{C}$ pairs gated by the $Q_3 = -7.16$ MeV band. The angular correlations in Figs. 7(a) and (b) were measured at a bombarding energy of 65 MeV, while the angular correlation shown in Figs. 7(c) and (d) were made at 77 and 87.4 MeV, respectively. The cross sections rise fairly dramatically over this energy

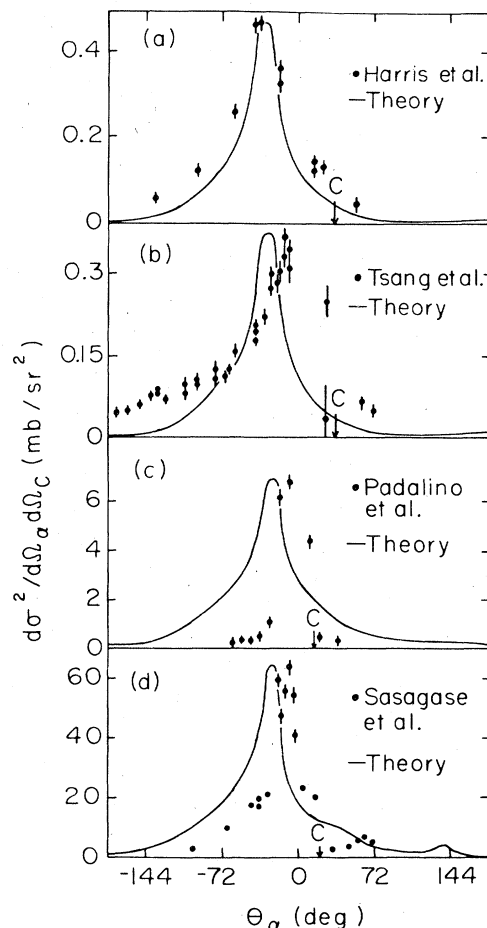


FIG. 7. The predicted and measured in plane angular correlations for $\alpha + \text{C}$ are given for bombarding energies of 65, 65, 77, and 87.4 MeV, respectively. The carbon detection angle is designated by an arrow.

range. However, it should be recognized that the 65 MeV data contain approximately half the strength of the angular correlation cross section because only the $Q_3 = -7.16$ MeV band is presented.

Using the measured 15° inclusive spectrum at 77 MeV

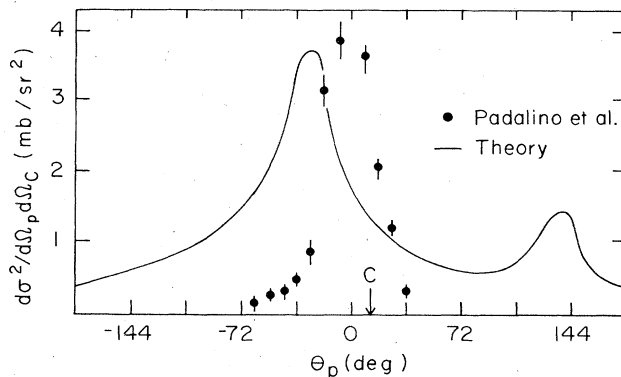


FIG. 8. The predicted and measured angular correlation for $p + \text{C}$ at 77 MeV.

and the 20° inclusive spectrum at 87.4 MeV, MCHF calculations were performed. The predictions of these calculations are shown in Figs. 7(c) and (d). At 65 MeV no 30° inclusive spectrum was readily available. Therefore, it was necessary to estimate one. A model, originally used by Serber¹⁴ to describe deuteron breakup, was modified^{1,2} and used to generate a 30° ¹²C inclusive spectrum for a bombarding energy of 65 MeV. Using the resulting ³¹P spectrum, MCHF calculations were performed [Figs. 8(a) and (b)]. All four predictions were normalized to the data.

With the exception of Harris's data, all three predicted angular correlations peaked farther out in angle than the measured angular correlations. Attempts to add excited states of ¹²C to the calculation further shifted the predicted peak back in angle. Thus, the best predictions were produced by only including ¹²C ground states.

The general shape and peak position of the predicted angular correlation is determined by many factors. The strongest factors are those of the separation energy between the alpha and ²⁷Al pair, the alpha evaporation distribution in the ³¹P reference frame, the low energy cutoff, and the ³¹P spectrum. The latter of these factors is dependent upon the carbon inclusive spectrum. The addition of ¹³C isotopes to the ¹²C spectrum causes the carbon distribution to shift up in energy, which would be higher than expected with a pure ¹²C distribution. This in turn produces a ³¹P excitation distribution which has been shifted lower in excitation energy causing the predicted angular correlation to peak farther out in angle. However, this effect appears to be small, based on the findings of Mikumo,¹⁵ the ¹³C cross sections at the forward angles are four to five times smaller than the ¹²C cross sections. Furthermore, when the ¹³C energy distribution is added to the ¹²C distribution, only a slight shift occurs in the ¹²C distribution. Thus ¹³C isotopes have little effect on the predicted angular correlations. The contributions to the experimental coincident $\alpha + ^{12}\text{C}$ cross sections due to ¹³C + α coincidences, which were produced from the ¹³C_{g.s.} + $\alpha + ^{26}\text{Al}_{g.s.}$ three-body final state, can be estimated from the Q_3 spectrum (Fig. 3). Q_3 values for the above three-body final state begin at $Q_{ggg} = -27.78$ MeV and become more negative for excited states in ¹³C and ²⁶Al. The absence of Q_3 peaks in the range from -27.78 MeV and below, indicates that the $\alpha + ^{13}\text{C}$ coincidences occur very infrequently.

In the present experiment at 77 MeV the angular range of the ³¹P* states prior to evaporation were generated from the ¹²C spectrum (Fig. 3). If the ³¹P* states are populated as inferred by Fig. 4 then we would expect the experimental angular correlation to peak near the centroid of the ³¹P distribution (between 30° and 40°). This corresponds to the most strongly populated states in the inferred ³¹P* spectrum (Fig. 4). However, this is not the case: the experimental peak occurs near -9° (Table II). The forward peaking of the angular correlation could occur if alpha decay was preferred over proton and neutron decay in the 35–45 MeV excitation range. This would leave the lower excitation energies to decay by single nucleon decay. If such a selectivity exists then the ³¹P spectrum would be divided into an alpha decay region and

TABLE II. The measured and calculated peak positions for the $\alpha + \text{C}$ angular correlations shown in Fig. 7.

Energy (MeV)	Measured	Calculated
65 ^a	-40°	-30°
65 ^b	-10°	-30°
77 ^c	-9°	-25°
87.4 ^d	-9°	-27°

^aReference 4.

^bReference 5.

^cThis work.

^dReference 3.

a proton and neutron decay region. The single nucleon decay region is more strongly populated than the alpha decay region; this would produce p-¹²C angular correlations which should have much larger cross sections than that of the $\alpha + ^{12}\text{C}$ correlations. Furthermore, the p-¹²C angular correlation should peak in the 30–40 deg angular range in the laboratory. Examination of the measured p-¹²C angular correlation (Fig. 8) does not support the above hypothesis. The $\alpha + ^{12}\text{C}$ and p + ¹²C angular correlations both peak at approximately the same angle. This would not be the case if the lower ³¹P* excitation energies favored p and n decay.

The positions of the $\alpha + ^{12}\text{C}$ and p + ¹²C angular correlation peaks and their relative strengths suggest that the incomplete fusion model presented here is not entirely correct. It is clear from energy conservation that the formation of ³¹P below 9 MeV excitation (corresponding to ¹²C energies > 66 MeV) does occur. However, ¹²C nuclei having energies below 66 MeV could also be observed in coincidence with alphas via inelastic breakup, or alpha emission from a nonequilibrated ³¹P. Either process could in principle produce forward peaking in the $\alpha + ^{12}\text{C}$ angular correlation. Certainly a broad base angular correlation could be explained by incomplete fusion (as presented by the calculations here) if one were to renormalize the predicted cross sections to a much lower value, but the sharply forward peaked part of the angular correlation must be produced via another mechanism.

Inelastic breakup could be producing the forward peaking, however, the present experiment was designed to enhance the observation of particles produced via IB, by placing the ¹²C detector inside the grazing angle. The inelastically scattered ¹⁶O nuclei, which have laboratory trajectories greater than 15°, prior to inelastic breakup will only produce $\alpha + ^{12}\text{C}$ coincidences in the alpha detector if it is placed beyond 15°. Thus, it would be expected that events measured in the 20°–40° range could be produced by IB. It is difficult to ascertain with any degree of confidence if IB occurs at 77 MeV, since the cross sections in this angular range are small. The small cross sections in the 20°–40° angular range limits the usefulness of kinematic tests in determining which reference frame the $\alpha + ^{12}\text{C}$ pair was produced from. The lack of strong evidence for inelastic breakup and the relative kinetic energy plots at 65 and 77 MeV support the hypothesis that pre-equilibrium decay rather than inelastic breakup occurs at this energy. At 87.4 MeV the relative kinetic energy,

measured over a small angular range of -15° to 10° , suggests that inelastic breakup is occurring at that energy. Presently, it would be difficult to speculate on the relative strengths of the two mechanisms as a function of bombarding energy without performing more detailed experiments on this system. However, it is evident from the data that both mechanisms occur and that the strengths of these mechanisms are dependent on the energy.

The difference between Harris's work and Tsang's work has not been resolved here. However, the systematics of the data measured at 77 and 87.4 MeV (Ref. 3) tends to support Tsang's findings. Our calculation agrees well with the anomalous data of Harris *et al.*,⁴ but does not reproduce the data at other energies in this system. Harris's data peak near the most probable direction for a ^{31}P intermediate state, thus it is not surprising that our model does a fairly good job of predicting Harris's data.

VI. SUMMARY

Projectile fragmentation in the $^{27}\text{Al}(^{16}\text{O},xy)$ reaction at 77 MeV was studied through angular correlation measurements between projectilelike fragments and alpha particles. Angular correlation measurements ranging over $+50^\circ$ to -63° (^{12}C detection at $\theta=15^\circ$) revealed little change in the shape of the angular correlation when compared to other studies. The relative kinetic energies between the final three-body state $\alpha + ^{12}\text{C} + ^{27}\text{Al}$ were calculated for the 77 MeV data, and found to be constant for the $\alpha + ^{27}\text{Al}$ pair. This suggests that a ^{31}P intermediate

state was formed. We have attempted to predict angular correlations between α - ^{12}C pairs at bombarding energies 67, 77, and 87.4 MeV. Presently, IB contributions to the angular correlation have not been included in the calculation. Our predictions reproduce the shape of the measured angular correlation fairly well. It was found that the predicted peak in the angular correlation was too far backward in angle when compared with the data at two of three energies. Since the position of the peaks is determined in our model by energy and momentum conservation, this disagreement suggests that another mechanism is occurring. At 65 MeV two sets of data exist and our calculations agree with one of the measured angular correlations but not the other. It is thought that inelastic breakup of ^{16}O or preequilibrium decay of ^{31}P may be causing the forward peaking in the α - ^{12}C angular correlation measurements. Measured relative kinetic energy plots produced at 65 and 77 MeV tend to support the preequilibrium mechanism over inelastic breakup at these energies. No explanation of the discrepancies between Harris's and Tsang's work is given here, but the systematics of the measurements made at 77 and 87.4 MeV support Tsang's findings.

ACKNOWLEDGMENTS

We would like to acknowledge R. Parker for his assistance in taking data. This work was supported in part by the National Science Foundation and the Florida State University.

-
- ¹S. L. Tabor, L. C. Dennis, and K. Abdo, *Phys. Rev. C* **24**, 2552 (1981).
²S. L. Tabor, L. C. Dennis, K. W. Kemper, J. D. Fox, K. Abdo, and G. Neushaefer, *Phys. Rev. C* **24**, 960 (1981).
³M. Sasagase, M. Sato, S. Harashima, K. Furuno, Y. Nagashima, Y. Tagishi, S. M. Lee, and T. Mikumo, *Phys. Rev. C* **27**, 2630 (1983).
⁴J. W. Harris, T. M. Cormier, D. F. Geesaman, L. L. Lee, Jr., R. L. McGrath, and J. P. Wurm, *Phys. Rev. C* **38**, 1460 (1977).
⁵M. B. Tsang, W. G. Lynch, R. J. Puigh, R. Vandenbosch, and A. G. Seamster, *Phys. Rev. C* **23**, 1560 (1981).
⁶W. D. M. Rae, A. J. Cole, B. G. Harvey, and R. G. Stockstad, *Phys. Rev. C* **30**, 158 (1984).
⁷T. Fukuda, M. Ishihara, M. Tanaka, I. Miura, H. Ogata, and H. Kamitsubo, *Phys. Rev. C* **25**, 2464 (1982).
⁸T. Udagawa, H. Frohlich, M. Ishihara, and K. Nagatani, *Phys. Rev. C* **20**, 1949 (1979).
⁹E. Takada, T. Shimoda, N. Takahashi, T. Yamaya, K. Nagatani, T. Udagawa, and T. Tamura, *Phys. Rev. C* **23**, 772 (1981).
¹⁰M. Sato, M. Sasagase, Y. Nagashima, J. Schimizu, T. Nakagawa, Y. Fukuchi, and T. Mikumo, *Phys. Rev. C* **27**, 2621 (1983).
¹¹J. Gomez del Campo, R. G. Stokstad, J. A. Biggerstaff, R. A. Dayras, A. H. Snell, and P. H. Stelson, *Phys. Rev. C* **19**, 2170 (1979).
¹²D. Glas and U. Mosel, *Nucl. Phys. A* **237**, 429 (1975).
¹³T. Ericson and V. Strotinski, *Nucl. Phys.* **8**, 284 (1958).
¹⁴R. Serber, *Phys. Rev.* **72**, 1008 (1947).
¹⁵T. Mikumo, M. Sasagase, M. Sato, T. Ooi, Y. Higashi, Y. Nagashima, and M. Yamanouchi, *Phys. Rev. C* **21**, 620 (1980).
¹⁶J. W. Harris, P. Braun-Munzinger, T. M. Cormier, D. F. Geesaman, L. L. Lee, Jr., R. L. McGrath, and J. P. Wurm, in *Proceedings of the International Conference on Nuclear Structure, Tokyo, 1977*, edited by T. Marumori (Physical Society of Japan, Tokyo, 1978), p. 698.